

2D Active Antenna Array Design for mMIMO to Improve Spectral and Energy Efficiency

Atul Kumar*, Jens Bartelt[†], Andre Noll Barreto[‡], and Gerhard Fettweis*

*Vodafone Chair Mobile Communications Systems Technische Universitat Dresden, Germany

Email: atul.kumar, gerhard.fettweis@tu-dresden.de

[†]Airrays GmbH, Dresden, Germany.

Email: jens.bartelt@airrays.com

[‡]Barkhausen Institut gGmbH - Würzburger Str, Dresden, Germany.

Email: andre.nollbarreto@barkhauseninstitut.org

Abstract—One of the aims of beyond 5G (B5G) wireless communication networks is to increase the data rates, while keeping lower latency and high energy efficiency. To achieve this, massive multiple-input-multiple-output (mMIMO) systems combined with two dimensional (2D) active antenna array (AAA) design are expected to play a key role. The main objective of this paper is to design a 2D-AAA with beamforming both in azimuth and elevation directions in order to improve the spectral efficiency and energy efficiency. Furthermore, we evaluate the impact of the designed 2D-AAA on the signal-to-interference-plus-noise ratio (SINR) performance by considering the 3D channel model given by 3GPP in the Urban Micro scenarios (UMi). For the design of 2D-AAA we consider 64 cross polarized antenna elements that are arranged as an 8-by-8 array, in which, at each column are stacked together pairwise to form sub-arrays. Therefore, transmit/receive (T/R) module, control circuitry and other RF processing unit are dedicated at a sub-array basis, and, due to this fewer components are required. Therefore, the cost of the 2D-AAA design is reduced. However, with the sub-arrays, the performance is degraded in terms of the side lobe level (SLL) when steering the main beam in other directions. In this contribution, we demonstrated that by proper designing of the 2D-AAA with optimal sub-array amplitude and phase tapering, it is possible to reduce the SLL. Moreover, due to the reduction of the SLL, an increase in spectral efficiency and SINR performance can be obtained.

Index Terms—Massive multiple-input-multiple-output; Beamforming; Spectral efficiency; Energy efficiency; Hybrid beamforming; Phased array antenna; Capacity; signal-to-interference-plus-noise ratio.

I. INTRODUCTION

To achieve high data-rates and capacity, which are key requirements for fifth generation communication systems (5G) and also for Beyond 5G (B5G), massive multiple-input-multiple-output (mMIMO) based on two dimensional (2D) active antenna arrays (AAAs) is a promising solution [1]. Moreover, mMIMO with 2D-AAA system is one of the candidates to realize high spectral efficiency for frequencies below 6 GHz and to enhance the coverage [2].

One of the main challenges to build mMIMO systems in practice is that the number of antennas that can be equipped at a base station (BS) is often limited by the BS form factors and by the operating carrier frequencies. LTE Release-13 leveraged the capacity of a mMIMO system by considering 64 antenna

elements [3]. Moreover, in Release-14, up to 256 antennas elements are considered and the number of the antenna elements is expected to further increase in the future to enhance the coverage [4]. However, with the increase of the antenna elements, the overhead to estimate the channel becomes quite significant. Furthermore, the required number of base-band chains, *i.e.*, transmit/receive (T/R) modules dedicated to each element increases, and, therefore, the cost is also higher [5].

To reduce the cost, a group of antenna elements can be stacked together to form a sub-array, and T/R modules, control electronic, communication interfaces, etc, can be shared for all elements in each sub-array. This provides a significant cost reduction, when compared with a mMIMO array in which each element is individually controlled [6]. Hence, each sub-array has a single digital phase and amplitude, which together with the large distance between the elements limits the steering. This means that the sub-arrayed antenna configuration has a limited steering capability steering capability of the overall antenna array for a specific side lobe level (SLL) [7].

In this paper, our goal is to design a 2D-AAA based on sub-arrays for a mMIMO system, such that the steering capability is increased and the SLL lowered. The lower SLL increases spectral efficiency and SINR performance by reducing intra and intercell interference, which can be shown by a system-level SINR analysis. This will be shown using the 3D channel model given by 3GPP for Urban Micro scenarios (UMi). The main contributions of this paper are:

- Optimized 2D-AAA design based on sub-arrays for reduced cost and improved spectral efficiency.
- Analysis of the impact of different window functions on the pattern and power efficiency of 2D-AAAs.
- SINR performance evaluation of the proposed 2D-AAA over a 3D channel model in UMi scenarios

The rest of this paper is organized as follows. A mathematical analysis of 2D-AAA design is presented in Section II, the design of the 2D-AAA based sub-array configuration is presented in Sec. III. Furthermore, the synthesis of the array pattern is given in Section IV, and the impact of the designed 2D-AAA in terms of SINR performance is shown in Section V, by considering a 3D channel model in the Urban Micro

scenario. Finally, conclusion and future works are discussed in Section VI.

II. FAR FIELD ANALYSIS OF 2D-AAA SYSTEM

In this section we analyse the far-field antenna radiation pattern $F(\theta, \phi)$ of a 2D AAA. It can be written as

$$F(\theta, \phi) = EP(\theta, \phi) \times AF_{sub-array}(\theta, \phi) \times AF_P(\theta, \phi), \quad (1)$$

where $EP(\theta, \phi)$ represents the response of each antenna element. The elements are assumed to have a cosine antenna pattern, written as

$$EP(\theta, \phi) = \cos^m(\theta)\cos^n(\phi) \quad (2)$$

with ϕ being the azimuth angle and θ the elevation angle. m and n are the exponents ≥ 0 . Larger exponent values narrow the response pattern of the element and increase the directivity.

Similarly, $AF_{sub-array}(\theta, \phi)$ is the field pattern of the sub-array. Here, control is provided within the sub-array, and the field pattern response with R elements can be written as

$$AF_{sub-array}(\theta, \phi) = \sum_{r=1}^R a_r e^{j\frac{2\pi}{\lambda} z_r \sin(\theta)} a_r e^{-j\frac{2\pi}{\lambda} z_r \sin(\theta_o)} \quad (3)$$

where a_r denotes the excitation amplitude, z_r the spacing between the elements in a sub-array, and θ_o the antenna elevation angle.

Moreover, $AF_P(\theta, \phi)$ is the array factor (AF), which for S sub-arrays is given as

$$AF_P(\theta, \phi) = \sum_{s=1}^{S=N_c \times N_r} c_s e^{j\frac{2\pi}{\lambda} y_s \cos(\theta)\sin(\phi) + z_s \sin(\theta)} e^{-j\frac{2\pi}{\lambda} y_s \cos(\theta_o)\sin(\phi_o) + z_s \sin(\theta_o)} \quad (4)$$

where c_s denotes the amplitude, y_s, z_s denotes the position of 2D-AAA, that is placed in Y-Z plane and it is radiating in the X direction, *i.e.* antenna array broadside is towards positive X-axis, N_r and N_c being the number of rows and columns of the antenna array, respectively. The resultant pattern of the 2D-AAA based on sub-array antenna can be obtained as shown in Fig. 1, using the simulation parameters related to elements and 2D-AAA design given in Table I. Since the patterns are plotted in logarithmic scale, the resultant sub-arrayed pattern shown is given by addition of element pattern, sub-array pattern, and array factor. From Fig. 1, it is clearly visible that the response of the array factor has a major impact on the SSL, *i.e.* the level of the highest side lobe in the pattern, relative to the main lobe $\rho = |A_{side}|/|A_{main}|$. A sidelobe will in general create interference for users outside the direction of the main lobe and has hence a major impact on cell-wide interference levels. Moreover, due to discrete phase shifts the ideal linear phase curve for electronic steering is approximated by a stair-step phase curve and this approximation results in a saw-tooth error curve. These periodic phase errors produce higher side lobes called as quantization lobes (QL) in the far-field patterns [12].

There are many techniques available in the literature to compensate the QL (that leads to higher steering range) [9]. The most common way to compensate QL are to place a phase

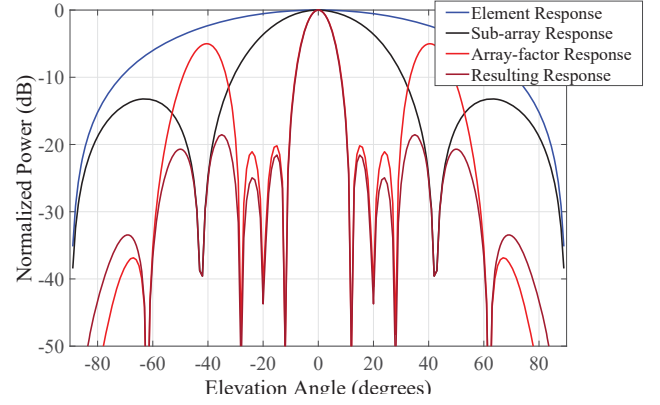


Fig. 1. Representation of the pattern multiplication effect for 2D-AAA design.

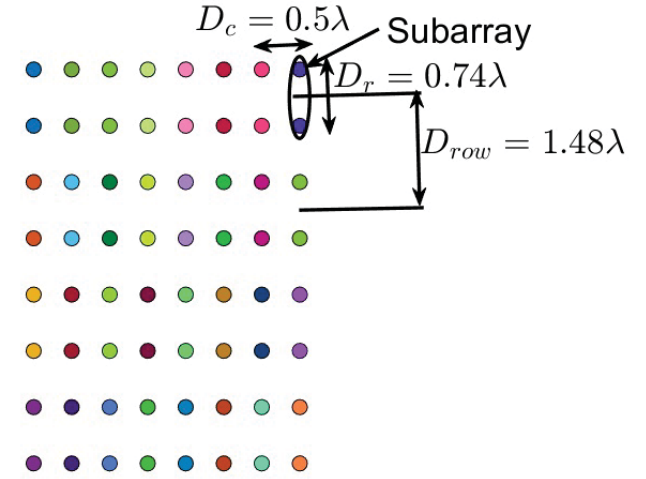


Fig. 2. Front view of regular 2D-AAA design for the mMIMO system where two elements are stacked together to form a sub-array.

shifter behind each antenna element, so as to steer the sub-array to the same direction as the main array. Although it increases the cost, it provides a big saving compared to the array with full degree of freedom because the T/R switches are only needed at the sub-array level.

Therefore, the array factor is the most important component to take into account in the design of the 2D-AAA system. From the pattern given in Fig. 1, we can observe two degrees of freedom to minimize the SLL. One is by choosing the antenna element that has narrower vertical half-power beamwidth (V-HPBW) and another is by increasing the distance between the elements in a sub-array.

Moreover, another approach to reduce side lobe is by redistributing the energy in the SLL throughout the far field pattern as this would break the periodicity of the phase errors, which is one of the reason for appearance of SLL. One approach to break the periodicity is by displacing either rows/columns of the planar array. So, by using row/column staggering together with the above two degrees of freedom, SLL may be reduced [12].

TABLE I
MAIN NOTATIONS AND SETTINGS OF SIMULATION PARAMETERS

Parameter	Value
Antenna elements and sub-array characteristics:	
Cosine antenna elements exponents (m, n)	$m=1.5, n=1.3$
3-dB beamwidth in azimuth direction (ϕ_{3dB})	104°
3-dB beamwidth in elevation direction (θ_{3dB})	93.5°
Azimuth and elevation angles (ϕ, θ)	$\phi \in [-360^\circ:360^\circ], \theta \in [-180^\circ:180^\circ]$
Carrier frequency (f_c)	2.5GHz
Wavelength (λ)	0.12m
2D Active Antenna Array design based on sub-array:	
Total number of sub-arrays (N_{tot})	32
Number of rows antennas (N_r)	4
Number of columns antennas (N_c)	8
Spacing between the row (D_{row})	1.48λ
Spacing between the columns (D_c)	0.5λ
Spacing between the elements in the sub-array (D_r)	0.74λ
Stagger distance for staggered (d_{sta})	0.87λ
Amplitude Tapering (w_i)	Different functions
Channel parameters for Urban Micro cell (3D-UMi)	
Scenarios	3D-UMi
Antenna configurations	1) Regular; 2) Staggered 2D-AAA
Downtilt	0° electrical tilt
BS antenna height	10m
Total BS Tx Power	41dBm
Number of BS	1
Number of sector per BS	3
Number of UE	8
UE height	1.5m
Position of UE	Fixed
UE antenna pattern	Isotropic antenna pattern
SINR performance evaluation parameter:	
Link between BS and UE	LOS
Receiver	Ideal channel estimation
Duplex	FDD
System bandwidth	10MHz
BS height	10m
Scenario	UMi

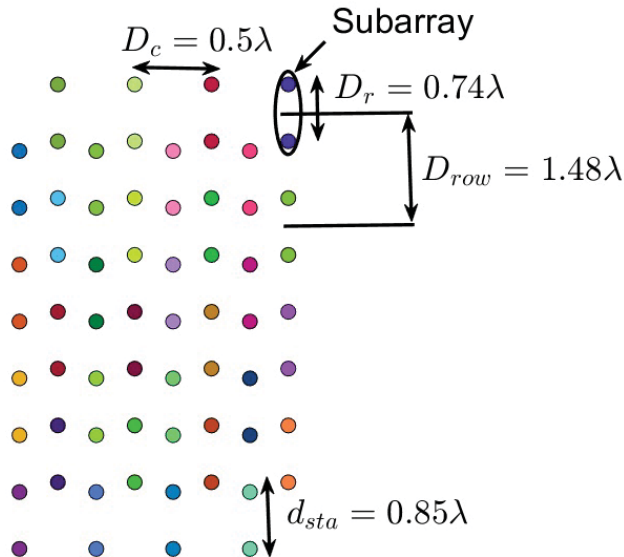


Fig. 3. Front view of staggered 2D-AAA with staggering alternative column of the array design for mMIMO system where two elements are stacked together to form a sub-array.

III. DESIGN OF 2D-AAA BASED ON SUB-ARRAY

In order to design the antenna array for a typical LTE carrier frequency of 2.5 GHz, fitting 32 antenna elements with

0.5λ spacing in a linear 1D-array, would require a horizontal room of 1.9m, which is still not feasible in many BS that has only limited room on the tower. Also, 1D-arrays provide beamforming capabilities in only one dimension. Therefore, in order to realize the benefits of mMIMO, an efficient implementation of 2D-AAA is a key requirement [7].

In 2D-AAA design, the gain and phase of the transmitted beam are controlled dynamically by digitally adjusting the excitation current applied to the active components. Another benefit of 2D-AAA is that it can accommodate a large number of antenna elements without increasing the deployment space [7]. Arranging these active antenna elements in a 2D array allows for the dynamic adaptation of the radiation pattern in both azimuth and elevation planes, making it possible to control the radio wave in the 3D space, in what is known as 3D beamforming [10].

In our 2D-AAA design, we consider 32 sub-arrays, by following same notation from Table I, where $N_c = 8$ with $D_c = 0.5\lambda$ and $N_r = 4$ with $D_r = 0.74\lambda$ representing the spacing between elements of the sub-array. The spacing between the adjacent sub-arrays is fixed denotes as $D_{row} = 1.48\lambda$ at 2.5 GHz operating frequency. This results in a size for the 2D-AAA of 0.42m horizontally and 0.621m vertically, that could comfortably fit on a macro-cell BS tower.

In this paper, we consider two different designs for the sub-array-based 2D-AAA mMIMO system represent as regular and staggered 2D-AAA configuration. Our main motivation is to analyse the impact of design interns of the SLL with steering capability in the 3D beamforming and furthermore on the SINR performance evaluation using 3D channel model in the UMi environments. Details of both Types of 2D-AAA design are given below:

- **Regular Configuration:** Figure 2 shows the front view of the regular 2D-AAA configuration, with the sub-array configuration. It consists in total of 64 cross polarized antenna elements¹ that are arranged as an 8-by-8 array. In each column, two elements are stacked together to form a sub array, and the elements of the sub-array are represented by the circles with same color. Therefore, 64 antenna elements are divided in 32 sub-arrays.
- **Staggered Configuration:** Figure 3 shows the front view of the staggered 2D-AAA configuration with alternating staggered columns, also with a sub-array configuration. The aim of the staggered configuration is to reduce QLs as explained earlier. As mentioned before, this can help reduce the SLL.

IV. 2D- ACTIVE ANTENNA ARRAY PATTERN SYNTHESIS

Based on the motivation of Sec. III, in this Section, we describe the pattern synthesis of the regular and staggered 2D-AAA design.

A. Regular Configuration

Here, we perform the antenna pattern synthesis and measure the SLL, while steering the main beam in different directions.

¹Conventionally there are twice the numbers of elements, half for one and half for the other polarization

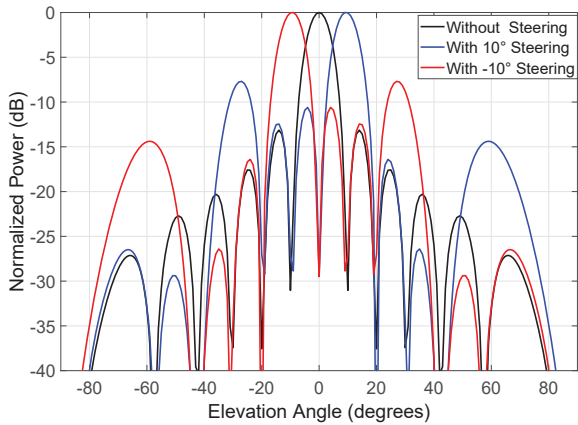


Fig. 4. Antenna array pattern synthesis results for the regular configuration with and without steering.

By doing this, we evaluate the steering capability of the designed 2D-AAA with 3D beamforming.

Figure 4 shows the pattern synthesis results of the regular configuration of 2D-AAA based on the simulation parameters given in Table I. From the results it is clearly visible that SLL is at a level around -10 dB, that further increases while steering the main beam in the other directions. As an example, at 10° the SLL level is around -6 dB. Due to this, the steering capability of the sub-array-based 2D-AAA design for the mMIMO system is limited by the increased SLL.

In order to reduce the SLL, in the literature, there are several methods available [8]. The most popular technique is to taper the amplitude using different window functions such as Hamming, Kaiser, Chebyshev, among others [11]. In tapering main task is to calculate an appropriate weights vector, which can reduce the SLL while steering the main beam in different directions. By applying different window functions, the resulting patterns are shown in Fig. 5. From the results it is clearly visible that, by using the different windows functions, SLL is reduced at some extent, where the Taylor window gives the better results compared with other window functions. Moreover, we can observe that the choice of a different window function alone is not a sufficient tool to reduce the SLL for a sub-array based 2D-AAA. In Table II, we compare the SLL performance of the different window functions at different steering angles.

However, applying window functions reduces the overall available power, which has a negative impact on the system coverage and range. Therefore, efficiency, E , is used as an evaluation parameter to determine how efficiently the input power is delivered at the output as

$$E = \frac{P}{P_{max}} = \frac{\sum_{i=1}^{N_{tot}} |w_i|^2}{N_{tot}}, \quad \forall |w_i| < 1. \quad (5)$$

where w_i corresponds to the weight of each sub-array and $N_{tot} = N_r \times N_c$ is the total number of sub-arrays. By comparing the different window functions, we can see from the Table II that the Taylor window gives the best solution for power efficiency and also in terms of SLL.

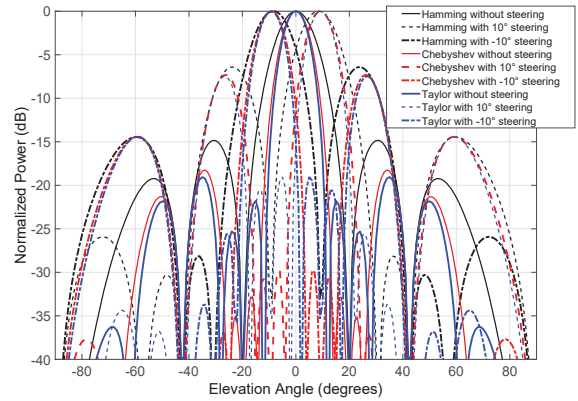


Fig. 5. Antenna array pattern synthesis results for different window function based on regular configuration with and without steering.

TABLE II
COMPARISON OF DIFFERENT WINDOW FUNCTION WITH POWER EFFICIENCY AND CORRESPONDING SLL FOR REGULAR 2D-AAA DESIGN

S.No	Different window function	% Power efficiency	$\rho = A_{side} / A_{main} $		
			With 0° Steering	With 10° Steering	With -10° Steering
1	Hamming	42.50	14.84	6.40	6.40
2	Kaiser	60.06	17.62	7.15	7.15
3	Chebyshev	71.45	18.24	7.31	7.31
4	Taylor	79.44	19.27	7.52	7.52

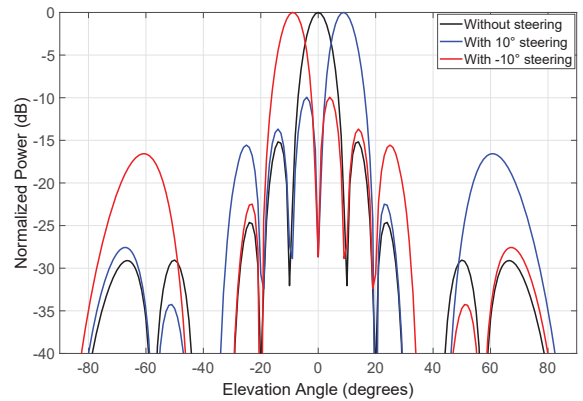


Fig. 6. Antenna array pattern synthesis results for the staggered configuration with and without steering.

B. Staggered Configuration

Here we evaluate the steering capabilities of the staggered configuration, as shown in Fig. 3.

Figure 6 and Table III show the antenna pattern synthesis results and it is clearly visible without windowing, SLL is lower than in the regular array, but still relatively high, but we can apply the same approach of different window functions to reduce the SLL further. The results are shown in Fig. 7, and we can see that due to staggering the columns, the SLL improves when compared with the regular configuration, with increased steering capabilities of the staggered configuration. Further-

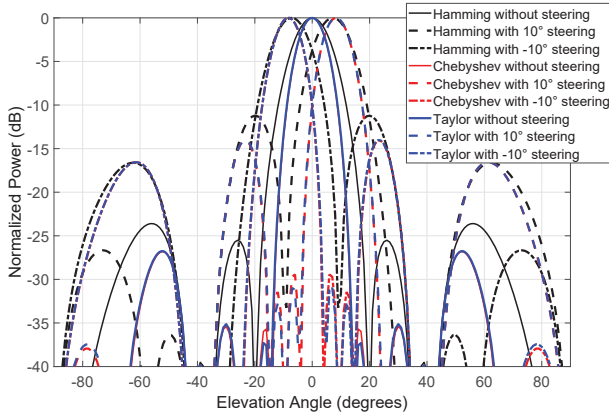


Fig. 7. Antenna array patterns synthesis results for different window function based on staggered configuration with and without steering .

TABLE III

COMPARISON OF THE DIFFERENT WINDOW FUNCTION WITH POWER EFFICIENCY FOR STAGGERED CONFIGURATION OF 2D-AAA DESIGN AND CORRESPONDING SLL

S.No	Different window function	% Power efficiency	$\rho = A_{side} / A_{main} $		
			With 0° steering	with 10° steering	with -10° Steering
1	Hamming	42.50	23.60	11.22	11.22
2	Kaiser	60.06	26.19	13.57	13.57
3	Chebyshev	71.45	26.84	14.07	14.07
4	Taylor	79.44	27.31	14.41	14.41

more, power efficiency of the different window functions is also given, computed based on the weight of the sub-array of the 2D-AAA design. By comparing the different window functions, we can see from the Table III, that Taylor window results in the highest power efficiency and lowest SLL, also for the staggered approach.

V. SINR PERFORMANCE ANALYSIS OVER 3D CHANNEL

After designing the different types sub-array based 2D AAA, in this section, we employ system level simulations based on the parameters given in Table I to analyse the SINR performance using the 3D channel model given by 3GPP for UMi scenarios [14].

As it is well known, 2D channel models are not adequate to evaluate the performance of 2D-AAA systems because they ignore the elevation parameters in describing the antenna patterns and propagation paths [15]. Accordingly, a three-dimensional spatial channel model (3D SCM) is considered by many authors in the literature [13]- [14], that takes into account azimuth as well as the elevation direction of signal propagation between a BS and a UE, such as the 3D channel model given by 3GPP and defined in the recent technical report TR 38.913 [13].

For this we are using the open-source Quadriga implementation of the 3D channel model [16]. However, a realistic performance assessment of mMIMO systems requires channel models that reflect the true behavior of the radio channel (*i.e.*, the propagation channel including effects of realistic antenna arrangements). 3D SCMs allow the separation of antenna and

Algorithm 1 Channel Coefficient Generation based on 3D-SCMs channel model for the downlink

- 1: Generate 2D-AAA with sub-arrays according to Sec.III.
- 2: Choose the designed 2D-AAA system (regular and staggered) to the BS and also assign omni directional antenna for UE.
- 3: Specify an environment to be simulated, such as suburban macro, urban macro, or urban micro specified by 3GPP.
- 4: Assign BS and UE location under the given UMi scenarios.
- 5: Setup the links such as line-of-sight (LOS) and non-line-of-sight (NLOS) between BS to each UE
- 6: Define other system parameter such as AOA and Small scale fading etc for UMi scenarios based on the technical report of 3GPP TR 38.913.
- 7: Run the simulation and generate 3D channel coefficient based on all sector of the antenna.

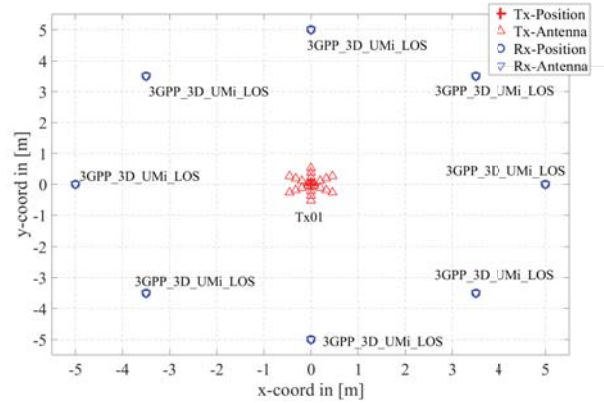


Fig. 8. Simulation setup to analyse the SINR performance using 3D channel model for different type of 2D-AAA design for mMIMO system.

propagation influences. Hence, they are ideal candidates for the evaluation of mMIMO systems since they are scalable in the spatial domain.

After modifying the simulation setup in QuaDRiGa channel model based on the parameters given in Table I, we generate the 3D channel coefficients that can be used further to evaluate the system level performance in terms of the SINR for different design of 2D-AAA system given in sec. III. In order to generate the channel coefficients, we follow the Algorithm 1 to setup the QuaDRiGa channel.

Figure 8 shows the positions of the different UE and BS in the simulated scenario. The link between each UE and the BS follows the simulation parameters given in Table I. Here, we consider 8 different UEs and each UE has one omni antenna at fixed location connected to a single BS with 3 sectors. Each sector contains a sub-array based 2D-AAA as given in Sec.III. Moreover, each UE is connected to BS with a direct LOS link. Our main motivation is to evaluate the SINR performance of different design of 2D-AAA configuration (regular and staggered) for the mMIMO system.

In Fig. 9 we show the cumulative distribution function

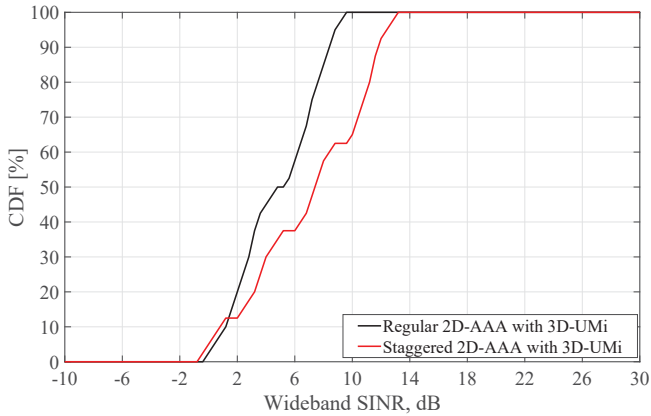


Fig. 9. CDF vs SINR performance analyses using the 3D channel model under the scenarios of UMi specified by 3GPP in TR 38.913.

TABLE IV

COMPARISON OF THE DIFFERENT ARRAY CONFIGURATIONS WITH TAYLOR WINDOW FOR FIXED STEERING BEAM WIDTH AND SIDE LOBE LEVEL

2D-AAA Design	SLL without Steering	SLL at 10° Steering	Steering beam width below 15dB SLL	SINR at 50% CDF
regular	19.27dB	7.52dB	5° → [-2.5° to 2.5°]	4.8dB
staggered	27.31dB	14.41dB	19° → [-9.5° to 9.5°]	7.5dB

(CDF) of the SINR based on the simulation parameters given in Table I. As it can be seen, the staggered array shows a higher SINR when compared with the regular one, due to its reduced SLL, which yields lower overall interference. Finally, Table. IV, shows that staggered configuration perform better as compared to regular configuration.

VI. CONCLUSION

Massive MIMO systems combined with 2D-AAA design are expected to play a key role for beyond 5G (B5G). In this paper, we show different configurations (regular and staggered) of a 2D-AAA mMIMO system and compare their SLLs, which are a main indicator for the steering capability. We also used different window functions to further reduce the SLL, and found that Taylor windows show the best results in terms of SLL and power efficiency. Moreover, we performed system-level simulations using the 3D channel model in the UMi scenarios based on the QuaDRiGa channel for mMIMO system. The results clearly showed that staggered performed better than regular ones in terms of SINR.

ACKNOWLEDGMENT

The research leading to this work was supported from the European Union's Horizon 2020 Research and Innovation Programme under Grant Agreement No. 762057 (5G-PICTURE). Neither the European Union nor its agencies are responsible for the contents of this paper; its contents reflect the views of the authors only.

REFERENCES

- [1] E. Björnson, L. Sanguinetti, H. Wymeersch, J. Hoydis, and Thomas L. Marzetta, "Massive MIMO is a Reality-What is Next? Five Promising Research Directions for Antenna Arrays," *arXiv preprint arXiv:1902.07678*, 2019.
- [2] Rakash SivaSiva Ganesan, *et al.*, "Integrating 3D channel model and grid of beams for 5G mMIMO system level simulations," in IEEE 84th Vehicular Technology Conference (VTC-Fall), pp. 1-6, Jan. 2016.
- [3] H. Ji and Y. Kim and J. Lee and E. Onggosanusi and Y. Nam and J. Zhang and B. Lee and B. Shim, "Overview of Full-Dimension MIMO in LTE-Advanced Pro," *IEEE Trans. on Wire. Comm.*, vol. 55, no. 2, pp. 176-184, Feb. 2017.
- [4] E. Björnson and J. Hoydis and L. Sanguinetti, "Massive MIMO Has Unlimited Capacity," *IEEE Trans. on Wire. Comm.*, vol. 17, no. 1, pp. 574-590, Jan. 2018.
- [5] I. Ahmed and H. Khammari and A. Shahid and A. Musa and K. S. Kim and E. De Poorter and I. Moerman, "A Survey on Hybrid Beamforming Techniques in 5G: Architecture and System Model Perspectives," *IEEE Comm. Sur. Tut.*, vol. 20, no. 4, pp. 3060-3097, Apr. 2018.
- [6] Y. Gao and T. Kaiser, "Antenna selection in massive MIMO systems: Full-array selection or subarray selection?," *IEEE Sensor Array and Multichannel Signal Processing Workshop (SAM)*, pp. 1-5, July 2016.
- [7] Qurat-Ul-Ain Nadeem and Abba Kammoun and Mohamed-Slim Alouini, "Elevation Beamforming with Full Dimension MIMO Architectures in 5G Systems: A Tutorial," *abs/1805.00225*, Jan. 2018.
- [8] U. Nickel, "Principles of adaptive array processing," Jan. 2016.
- [9] H. Kamoda and J. Tsumochi and F. Sugimoto, "Reduction in quantization lobes due to digital phase shifters for phased array radars," *Asia-Pacific Microwave Conference*, Dec. 2011.
- [10] Y. Nam and B. L. Ng and K. Sayana and Y. Li and J. Zhang and Y. Kim and J. Lee, "Full-dimension MIMO (FD-MIMO) for next generation cellular technology," *IEEE Comm. Mag.*, vol. 51, no. 6, pp. 172-179, June. 2013.
- [11] R. Haupt, *et al.*, "Reducing grating lobes due to subarray amplitude tapering," *IEEE Tran, on Ant. and Prop.*, vol. 33, no. 8, pp. 846-850, Aug. 1989.
- [12] H. Wang and D. Fang and Y. L. Chow, "Grating Lobe Reduction in a Phased Array of Limited Scanning," *IEEE Tran, on Ant. and Prop.*, vol. 56, no. 6, pp. 1581-1586, June. 2008.
- [13] 3GPP, "TR 36.873: Technical Specification Group Radio Access Network; Study on 3D channel model for LTE (Release 12)," 3GPP, Tech. Rep. V12.2.0, 2015.
- [14] 3GPP, "TR 36.897: Technical Specification Group Radio Access Network; Study on elevation beamforming / Full-Dimension (FD) Multiple Input Multiple Output (MIMO) for LTE (Release 13)," 3GPP, Tech. Rep. V13.0.0, 2015.
- [15] A. Forenza and D. J. Love and R. W. Heath, "Simplified Spatial Correlation Models for Clustered MIMO Channels With Different Array Configurations," *IEEE Transactions on Vehicular Technology*, vol. 46, no. 4, pp. 1924-1934, July 2007.
- [16] S. Jaeckel, "Quasi-deterministic channel modeling and experimental validation in cooperative and massive MIMO deployment topologies," *TU Ilmenau*, 2017.